Cryptococcus neoformans Chitin Synthase 3 (Chs3) Plays a Critical Role in Dampening Host Inflammatory Responses

Camaron R. Hole[a], Woei C. Lam[a], Rajendra Upadhya[a], and Jennifer K. Lodge[a#]

[a]Department of Molecular Microbiology, Washington University School of Medicine, St. Louis, MO, USA.

Running Head: Cryptococcal Chs3 impacts immune responses

#Address correspondence to Jennifer K. Lodge, lodgejk@wustl.edu

ABSTRACT:

Cryptococcus neoformans infections are significant causes of morbidity and mortality among AIDS patients and the third most common invasive fungal infection in organ transplant recipients. One of the main interfaces between the fungus and the host is the fungal cell wall. The cryptococcal cell wall is unusual among human pathogenic fungi in that the chitin is predominantly deacetylated to chitosan. Chitosan deficient strains of *C. neoformans* were found to be avirulent and rapidly cleared from the murine lung. Moreover, infection with a chitosan deficient *C. neoformans* lacking three chitin deacetylases (*cda1Δ2Δ3Δ*) was found to confer protective immunity to a subsequent challenge with a virulent wild type counterpart. In addition to the chitin deacetylases, it was previously shown that chitin synthase 3 (Chs3) is also essential for chitin deacetylase mediated formation of chitosan. Mice inoculated with *chs3Δ* at a dose previously shown to induce protection with cda*1Δ2Δ3Δ* die within 36 hours after installation of the organism. Mortality was not dependent on viable fungi as mice inoculated with heat-killed preparation of *chs3Δ* died at the same rate as mice inoculated with live *chs3Δ*, suggesting the rapid onset of death was host mediated likely caused by an over exuberant immune response. Histology, cytokine profiling, and flow cytometry indicates a massive neutrophil influx in the mice inoculated with *chs3Δ*. Mice depleted of neutrophils survived *chs3Δ* inoculation indicating that death was neutrophil mediated. Altogether, these studies lead us to conclude that Chs3, along with chitosan, plays critical roles in dampening cryptococcal induced host inflammatory responses.

IMPORTANCE:

Cryptococcus neoformans is the most common disseminated fungal pathogen in AIDS patients, resulting in ~200,000 deaths each year. There is a pressing need for new treatments for this infection, as current antifungal therapy is hampered by toxicity and/or the inability of the host's immune system to aid in resolution of the disease. An ideal target for new therapies is the fungal cell wall. The cryptococcal cell wall is different than many other pathogenic fungi in that it contains chitosan. Strains that have decreased chitosan are less pathogenic and strains that are deficient in chitosan are avirulent and can induce protective responses. In this study we investigated the host responses to *chs3*Δ*,* a chitosan-deficient strain, and found mice inoculated with *chs3*Δ all died within 36 hours and death was associated with an aberrant hyperinflammatory immune response driven by neutrophils, indicating that chitosan is critical in modulating the immune response to *Cryptococcus*.

Introduction:

Cryptococcus neoformans is a ubiquitous encapsulated fungal pathogen that causes pneumonia and meningitis in immunocompromised individuals. *C. neoformans* is the most common disseminated fungal pathogen in AIDS patients, with an estimated quarter million cases of cryptococcal meningitis each year resulting in ~200,000 deaths (1, 2) and remains the third most common invasive fungal infection in organ transplant recipients (3). Current antifungal therapy is often hampered by toxicity and/or the inability of the host's immune system to aid in resolution of the disease; treatment is further limited by drug cost and availability in the resource-limited settings (4). The acute mortality rate

of patients with cryptococcal meningitis is between 10-30% in medically-advanced countries (5, 6), and even with appropriate therapy at least one third of patients with cryptococcal meningitis will undergo mycologic and/or clinical failure (4). Patients that do recover can be left with profound neurological sequelae, highlighting the need for more effective therapies, and/or vaccines to combat cryptococcosis

One of the main interfaces between the fungus and the host is the fungal cell wall. Most fungal cell walls contain chitin, however, the cryptococcal cell wall is unusual in that the chitin is predominantly deacetylated to chitosan. Chitin is a homopolymer of β-1,4-linked *N*-acetylglucosamine (GlcNAc) and is one of the most abundant polymers in nature. Immunologically, chitin can induce allergy and strong Th2-type immune responses (7). Chitin is polymerized from cytoplasmic pools of UDP-GlcNAc by a multiple trans-membrane protein chitin synthase (CHS) and there are eight Chs's encoded in *C. neoformans* genome (8). Chitosan, the deacetylated form of chitin, is generally less abundant in nature than chitin, but is found in the cell wall of several fungal species depending on growth phase (8). Chitosan is not synthesized de novo but is generated from chitin through enzymatic conversion of GlcNAc to glucosamine by chitin deacetylases (CDAs) and *C. neoformans* makes three CDAs (9). Why *Cryptococcus* converts chitin to chitosan and what advantages this conversion provides to the organism are not well understood.

Deletion of a specific chitin synthase (CHS3), or deletion of all three chitin deacetylases causes a significant reduction in chitosan in the vegetative cell wall (9). These chitosan deficient strains of *C. neoformans* are avirulent and rapidly cleared from the murine lung (9). Moreover, infection with a chitosan deficient *C. neoformans* strain

lacking three chitin deacetylases (*cda1Δ2Δ3Δ*) was found to confer protective immunity to a subsequent challenge with a virulent wild type counterpart (10). These findings suggest that there is an altered host response to chitosan-deficient strains. Therefore, we wanted to determine the nature of host immune response to an infection with chitosan deficiency caused by the deletion of *C. neoformans CHS3* gene.

Surprisingly, we observed that all mice inoculated with chitosan-deficient *chs3Δ* died within 36 hours. Death was not dependent on live organism or the mouse background. We hypothesized that the rapid onset of mortality was likely due to an aberrant immune response. Histology, cytokine profiling, and flow cytometry indicates a massive influx of neutrophils in the mice inoculated with *chs3*Δ. Mice depleted of neutrophils all survived inoculation of the *chs3Δ* strain, indicating that the observed mortality is neutrophil mediated. Together, these results suggest that chitin synthase 3 is important in modulating the immune response to *Cryptococcus*.

Results:

Complete deletion and complementation of *C. neoformans* chitin synthase 3 (Chs3).

With better annotation of the cryptococcal genome, we found that our previously reported *chs3Δ* strain (8) was not a complete deletion. While the protein is not functional as the catalytic domain was deleted, the original strain still harbored 689 bp of gene sequence potentially sufficient to encode a ~25 kDa protein. As this gene is highly expressed under vegetative growth, the truncated protein might influence either the virulence or the nature of the host immune response to the mutant. Due to this, we generated a complete deletion of the chs3 gene, including the 5' UTR to delete the

promoter as well, in KN99 by biolistic transformation. All the isolates were characterized by diagnostic PCR screening and southern blot hybridization.

The original *chs3Δ* strain exhibited a large number of phenotypes including changes in morphology including 2-3 fold enlarged cells and a budding defect, temperature sensitivity, leaky melanin, and chitosan deficiency, among others (8). Cells of the new *chs3Δ* strain exhibited the same morphologic changes observed in the original strain (Fig. 1A). Additionally, the new *chs3Δ* strain is also temperature sensitive (Fig. 1B) and deficient in chitosan (Fig. 1C).

Previously we attempted to complement the original *chs3Δ* strain a multitude of ways and all attempts failed, leading us to conclude that the cell wall of the *chs3Δ* strain was compromised to a point that they could not survive any of the transformation procedures. (9). With this in mind, we attempted to complement the new *chs3Δ* strain using electroporation into the endogenous locus, replacing the NAT resistance marker and were successful. The complemented strain (*chs3Δ::CHS3)* reversed all the observed phenotypes including the changes in morphology, temperature sensitivity and chitosan deficiency (Fig. 1A-C).

Inoculation with the *chs3*Δ strain induces rapid mouse mortality.

We have previously shown that chitosan is essential for growth in the mammalian host. Strains with three different chitosan deficiency genotypes (*chs3*Δ, *csr2*Δ, and *cda1*Δ*2*Δ*3*Δ) all show rapid pulmonary clearance in a mouse model of cryptococcosis and complete loss of virulence (9). Mice that received a high inoculation (10^7 CFU) of the chitosan deficient strain *cda1*Δ*cda2*Δ*cda3*Δ were able to clear the infection and were

found to be protected against a subsequent challenge with wild-type KN99 (WT) *C. neoformans* (10). Notably, this chitosan deficient strain is protective even when heat-killed (10). Protective immunization is dependent on the inoculum size, as only mice that received 10^7 CFU of *cda1*Δ*cda2*Δ*cda3*Δ were protectively immunized, mice that received a lower inoculation were not protected (10).

Based on these data, we set out to test whether inoculation with other chitosan deficient strains would also confer protection. We started this process using the new *chs3*Δ strain which is chitosan deficient (Fig. 1C). We inoculated C57BL/6 mice intranasally with 10^7 CFU of live *cda1Δ2Δ3Δ* (a concentration that is shown to be protective for *cda1*Δ*2*Δ*3*Δ), *chs3*Δ, *chs3*Δ*::CHS3,* or WT *C. neoformans* KN99 and were monitored for survival. As expected, mice that received *cda1Δ2Δ3Δ* all survived the infection and mice that received the WT KN99 or *chs3*Δ*::CHS3* all died or were euthanized due to morbidity around day 6 (KN99) or day 8 (*chs3*Δ*::CHS3)* post inoculation with this high inoculum (Fig. 2). What was surprising, however, was that the mice inoculated with *chs3*Δ all died within 36 hours after instillation of the organism (Fig. 2).

The rapid rate of mortality suggested death was not due to fungal proliferation or burden. Furthermore, we previously showed that the original *chs3*Δ strain is rapidly cleared from the host at a lower inoculum (9). Based on these finding, we tested if mortality was dependent on viable fungi. We heat-killed (HK) WT KN99, *chs3*Δ*,* and *chs3*Δ*::CHS3* strains at 70°C for 15 minutes. Complete killing was confirmed by plating for CFUs. C57BL/6 mice then received an intranasal inoculation with 10^7 CFU of HK WT KN99, HK *chs3*Δ or HK *chs3*Δ*::CHS3* and were monitored for survival. Mice that received HK WT KN99 or HK *chs3*Δ*::CHS3* all survived the inoculation of heat killed cells (Fig. 3A).

Conversely, mice that received HK *chs3*Δ all died at the same rate as observed above with live *chs3*Δ (Figs. 2 and 3A) indicating that mortality was not dependent on the viability of the fungi. In addition, to confirm that the observed phenotype was due to loss of Chs3 and not some secondary mutation in the strain used, we assayed the original *chs3*Δ mutant strain (Supplemental figure 1) and saw the same rapid mortality observed in Figure 3A.

Different mouse backgrounds have various susceptibilities to *C. neoformans* depending on the strain used (11). Due to the strong phenotype observed with *chs3*Δ in the C57BL/6 mice, we wanted to verify that rapid rate of mortality was not due to the mouse background. To assess susceptibility in different mouse backgrounds, BALB/c or CBA/J mice received an intranasal inoculation with 10^7 CFU of HK WT KN99, HK *chs3*Δ or HK *chs3*Δ*::CHS3* and were monitored for survival. Regardless of the mouse background, mice that received HK WT KN99 or HK *chs3*Δ*::CHS3* all survived the challenge, whereas mice that received HK *chs3*Δ all died at the same rate as observed in the C57BL/6 mice (Figs. 3A-C) indicating that rapid rate of mortality was not a mouse background phenomenon.

A massive inflammatory response is triggered to *chs3*Δ inoculation.

The above data indicates that mice are not dying due to the fungal burden, as death was not dependent on viable fungi in multiple mouse backgrounds (Figure 3). These data suggest that the mortality associated with *chs3*Δ maybe host mediated (12). To test this, C57BL/6 mice received an intranasal inoculation with 10^7 CFU HK WT KN99, HK *chs3*Δ or HK *chs3*Δ*::CHS3* and the lungs were processed for histology. For all immune studies, we chose to use heat-killed fungi to control for fungal burden as the WT KN99

and *chs3Δ::CHS3* would rapidly outgrow the *chs3Δ* strain and potentially skew our results. Lungs were processed at 8 hours post inoculation as we could not constantly keep the *chs3Δ* inoculated mice alive for the full 24h. The 8-hour time point was chosen as this was the time the animal started to show signs of morbidity. The paraffin embedded lungs were sectioned and processed for hematoxylin-eosin (H&E) staining. Histological analysis of the infected lung show little pathology in the lung of the mice inoculated with either HK KN99 or HK *chs3Δ::CHS3* compared to the strong inflammatory response in the lungs of the *chs3Δ* inoculated mice at 8h (Figure 4). The lungs from mice inoculated with *chs3Δ* exhibit abundant foci of inflammation spread across the whole lung section (Fig 4C) consisting of a profound amount of mixed inflammatory infiltrates with enhanced presences of granulocytes (Figs 4D-E). Such severe pneumonia and lung damage could explain the mortality observed in *chs3Δ* inoculated mice and indicates that the immune response in the lungs, albeit robust, is nonprotective and detrimental.

***chs3Δ* induces a strong proinflammatory cytokine response.**

Because we observed massive infiltration of immune cells in the lungs of *chs3Δ* inoculated mice (Figs 4D-E), we next assessed the cytokine/chemokine produced. To do this, C57BL/6 mice received an intranasal inoculation with 10^7 CFU HK WT KN99, HK *chs3Δ* or HK *chs3Δ::CHS3* and at 8hr post inoculation homogenates were prepared from the lungs of each group as well as a PBS control group. Cytokine/chemokine responses were determined from the lung homogenates using the Bio-Plex Protein Array System. We observed an increase in multiple cytokines (Supplementary Figure 2), however there was a significant increase in the chemokines KC (Fig. 5A) and G-CSF (Fig. 5B), as well as extremally high levels of IL-6 (Fig. 5C) in *chs3Δ* inoculated mice compared to PBS,

185 HK WT KN99 or HK *chs3*Δ*::CHS3* inoculated mice. This cytokine profile is indicative of a
186 strong neutrophilic response in the lungs which correlates with the histology data above
187 indicating an enhanced presence of granulocytes (Figure 4).

188 **A significant increase in neutrophil recruitment in the lungs of *chs3*Δ inoculated**
189 **mice.**

190 Since both the histology and cytokine analysis indicates a strong inflammatory
191 response, we wanted to identify the responding cells. For this, C57BL/6 mice received an
192 intranasal inoculation with 10^7 CFU of HK WT KN99, HK *chs3*Δ or HK *chs3*Δ*::CHS3* and
193 at 8hr post inoculation pulmonary leukocytes were isolated from the lungs of each group
194 by enzymatic digestion and subjected to flow cytometry analysis for leukocyte identity
195 (Supplementary Figure 3). Consistent with the above histology data, there was a
196 significant increase in the total number of immune cells in the lungs of *chs3*Δ inoculated
197 mice (Fig. 6A). In addition, there was a significant increase in both the total number and
198 percent neutrophils in the lungs *chs3*Δ inoculated mice compared to the WT KN99 or HK
199 *chs3*Δ*::CHS3* inoculated mice (Figs 6B-C). We did not observe a significant change in
200 any of the other cell types assayed (Supplementary Figure 4).

201 **Depletion of neutrophils protects *chs3*Δ inoculated mice.**

202 Due to the significant increase in neutrophil recruitment to the lungs of mice
203 inoculated with the *chs3*Δ strain, we sought to determine the role of neutrophils in the
204 rapid mortality observed in these animals. To test this, C57BL/6 mice were injected with
205 200ug of anti-Ly6G (1A8), an antibody that specifically depletes neutrophils (13, 14)) or
206 an isotype antibody 24 hours before intranasal inoculation with 10^7 CFU of HK *chs3*Δ and

monitored for survival. Mice were injected with antibody every 24 hours for the first 5 days post challenge. After day 5, the mice were injected every 48 hours. This antibody is usually injected every 48 hours, however, with the high number of neutrophils recruited (Fig. 6) and the elevated levels of neutrophil growth factors (Fig. 5) we elected to increase the number of the initial injections to ensure neutrophil depletion. Mice treated with the isotype antibody all died at the same rate as observed above with HK *chs3*Δ (Figs. 3A and 7A), whereas mice that were treated with anti-Ly6G all survived (Fig. 7A) indicating that death was neutrophil mediated. To confirm this finding, we repeated the experiment in BALB/c and CBA/J mice. Consistent with our findings in C57BL/6, mice that were depleted of neutrophils all survived inoculation with HK *chs3*Δ whereas mice treated with the isotype antibody all died regardless of mouse background (Figs 7B-C). These data demonstrate that the rapid rate of mortality observed in mice inoculated *chs3*Δ is neutrophil dependent.

Discussion:

We have previously shown that deletion of a specific chitin synthase (CHS3), or deletion of all three chitin deacetylases causes a significant reduction in chitosan in the vegetative cell wall (9). These chitosan deficient strains of *C. neoformans* were found to be avirulent and rapidly cleared from the murine lung (9). Moreover, infection with a chitosan deficient *C. neoformans* strain lacking three chitin deacetylases (*cda1Δ2Δ3Δ*) was found to confer protective immunity to a subsequent challenge with a virulent wild type counterpart (10). These findings suggest that there is an altered host response to chitosan-deficient strains. Surprisingly, we observed that mice inoculated with chitosan-deficient *chs3*Δ all died within 36 hours (Figs. 2 and 3) and death was associated with an

aberrant hyperinflammatory immune response indicating that chitosan is critical in modulating the immune response to *Cryptococcus*.

The immune response to *Cryptococcus*, as well as the magnitude of the response, can play a protective or detrimental role. Our data fits well within the damage-response framework proposed by Casadevall and Pirofski (12) where host damage or benefit is dependent on the host response. This is represented as a parabolic curve, where too little of a response to a microorganism can lead to damage caused by the microorganism and to strong of a host response can lead to damage caused by the host response. This framework is observed in cryptococcal infected AIDS patients. Too little of a response can lead to patient death due to the fungus, whereas a hyperactive response can lead to death caused by immunopathology. AIDS patients treated with antiretroviral therapy often develop cryptococcal immune reconstitution inflammatory syndrome (IRIS) which is an exaggerated and frequently deadly inflammatory reaction that complicates recovery from immunodeficiency (15). Cryptococcal IRIS emphasizes the potential role of the host immune system in mediating host damage and disease symptoms.

There is precedent to study mutants that induce an aberrant hyperinflammatory immune response, as similar responses have been observed with cryptococcal IRIS. Cryptococcal IRIS develops in 8-49% of patients with known cryptococcal disease before antiretroviral therapy (16). The pathogenesis of IRIS is poorly understood, and prediction of IRIS is not currently possible. Innate immune cells, such as monocytes and neutrophils, are of increasing interest in IRIS pathophysiology, since granuloma appears to be frequently found in IRIS lesions (15). Additionally, at the time of IRIS onset multiple proinflammatory cytokine are detected, including IL-6 (17). Further study of the *chs3Δ*

immune response could advance our understanding of host immune mechanisms involved in an inappropriately strong immune response to *Cryptococcus,* like those seen in immune reconstitution inflammatory syndrome. These studies have the potential to advance our understanding of a significant problem in the management of cryptococcal patients.

Other cryptococcal mutants that have defects in the cell wall, like *rim101*Δ, have been found to induce a strong proinflammatory response and lead to neutrophil recruitment (18), however, not to the order of magnitude observed with *chs3Δ.* Neutrophils have a complicated role in the cryptococcal immune response. While neutrophils can kill *C. neoformans,* the fungus can modulate the neutrophil response. Cryptococcal capsular and cell wall components can inhibit neutrophil migration (19, 20), and can inhibit the production of neutrophil extracellular traps (21). In the brain, neutrophils have been shown to be important in clearance of the fungus from the microvasculature (22, 23). Neutrophil depletion in a protective immunization model did not affect pulmonary fungal burden, indicating that neutrophils are not required for clearance (13) or for the secondary response (14). These data further support the observation by Mednick et al. that neutropenic mice given a pulmonary *C. neoformans* infection survived significantly longer than control mice that had an intact neutrophil compartment (24), therefore indicating that neutrophils are not necessary for protective responses against cryptococcal infection. We observed a significant increase in neutrophil recruitment to the lungs of mice inoculated with the *chs3*Δ strain (Figs 6B-C). Mice inoculated with HK *chs3*Δ and depletion of neutrophils all survived whereas the isotype treated mice all died (Fig. 7), indicating a detrimental role of neutrophils. Further

supporting a harmful role for neutrophils, mice with genetically-induced neutrophilia appear to have increased susceptibility to cryptococcal disease (25). More work is needed to elucidate our understanding the cryptococcus:neutrophil interactions.

In summary, we have shown that inoculation with either live or dead cells from the chitosan deficient strain, *chs3*Δ, leads to death of the mice within 36 hours. The rapid on set of death is likely due to an aberrant hyperinflammatory immune response as mortality was not dependent on viable fungi. Histology, cytokine profiling, and flow cytometry indicates a massive influx of neutrophils in the mice inoculated with *chs3*Δ. Depletion studies show a damaging role for neutrophils in the response to *chs3*Δ. Altogether, chitosan plays a major role in the immune response to *C. neoformans.* In addition, the response to chitosan deficient *C. neoformans* seems to depend on the type of genes deleted, as not all chitosan deficient strains induce the same immune response.

Materials and Methods:

Fungal strains and media:

C. neoformans strain KN99α was used as the wild-type strain and as progenitor of mutant strains. Strains were grown in YPD broth (1% yeast extract, 2% bacto-peptone, and 2% dextrose) or on YPD solid media containing 2% bacto-agar. Selective YPD media was supplemented with 100 µg/mL nourseothricin (NAT) (Werner BioAgents, Germany).

Strain construction:

297 Gene-specific deletion construct of the chitin synthase 3 gene (CNAG_05581) was
298 generated using overlap PCR gene technology described previously (26, 27) and
299 included the nourseothricin resistance cassette. The primers used to disrupt the genes
300 are shown in Table S1. The Chs3 deletion cassette contained the nourseothricin
301 resistance cassette resulting in a 1,539 bp replacement of the genomic sequence
302 between regions of primers 3-Chs3 and 6-Chs3 shown in upper case in Table S1. The
303 construct was introduced into the KN99α strain using biolistic techniques (28). To
304 generate a *CHS3* complement strain, we replaced the NAT resistance cassette in
305 the *chs3* deletion strain with the native *CHS3* gene sequence by electroporation (29) and
306 screened for NAT sensitivity.

307 **Morphological analysis:**

308 Cells were incubated for 2 days in YPD medium at 30°C with shaking and diluted to an
309 OD_{650} of 0.2 with PBS. Five microliters each cell solution was spotted on to a clean glass
310 slide and photographed on an Olympus BX61 microscope.

311 **Evaluation of temperature sensitivity:**

312 Wild-type, *chs3* deletion and *chs3Δ::CHS3* complement strains were grown in liquid YPD
313 for 2 days at 30°C with shaking. Cells were diluted to OD_{650}=1.0 and 10-fold serial
314 dilutions were made. Five microliters of each dilution were spotted on YPD plates and the
315 plates were incubated for 2-3 days at 30°C and 39°C and photographed.

316 **Cellular chitosan measurement**:

317 As previously described, MBTH (3-methyl -2-benzothiazolinone hydrazone) based
318 chemical method was used to determine the chitin and chitosan content (30). In brief,

cells were grown in liquid YPD for 2 days at 30ºC with shaking collected by centrifugation. Cell pellets were washed two times with PBS, pH 7.4 and lyophilized. The dried samples were resuspended in water first before adding KOH to a final concentration of 6% KOH (w/v). The alkali suspended material was incubated at 80ºC for 30 min with vortexing in between to eliminate non-specific MBTH reactive molecules from the cells. Alkali treated material was then washed several times with PBS, pH 7.4 to make sure that the pH of the cell suspension was brought back to neutral pH. Finally, the cell material was resuspended in PBS, pH 7.4 to a concentration of 10mg/mL in PBS (by dry weight) and a 0.1 mL of each samples was used in the MBTH assay (31).

Mice:

BALB/c (000651), CBA/J (000656), and C57BL/6 (000664) mice were obtained from Jackson Laboratory (Bar Harbor, ME). BALB/c and C57BL/6 obtained from Jackson Labs are also known as BALB/cJ and C57BL/6 respectively. All mice were 6 to 8 weeks old at the time of inoculation. All animal protocols were reviewed and approved by the Animal Studies Committee of the Washington University School of Medicine and conducted according to National Institutes of Health guidelines for housing and care of laboratory animals.

Pulmonary inoculations:

Strains were grown at 30°C, 300 rpm for 48 hours in 50 mL YPD. The cells were centrifuged, washed in endotoxin-free 1x PBS and counted with a haemocytometer. For studies utilizing heat-killed organism, after being diluted to the desired cell number in PBS, the inoculum was heated at 70°C for 15 minutes. Complete killing was assayed by platting for CFUs. Mice were anaesthetized with an intraperitoneal injection (200 µL) of

ketamine (8 mg/mL)/dexmedetomidine (0.05 mg/mL) mixture and then given an intranasal inoculation with 1 × 10^7 CFU of live or heat-killed organism in 50 µl of sterile PBS. Anesthesia was reversed by an intraperitoneal injection of (200 µL) of antipamezole (0.25mg/mL). The mice were fed *ad libitum* and monitored daily for symptoms. For survival studies mice were sacrificed when body weight fell below 80% of weight at the time of inoculation. For cytokine analysis, flow cytometry studies, and histology, mice were euthanized at 8-hours post-inoculation by CO_2 inhalation and the lungs were harvested.

Histology:

Mice were sacrificed according to approved protocols, perfused intracardially with sterile PBS, and the lungs inflated with 10% formalin. Lung tissue was then fixed for 48 hours in 10% formalin and submitted to HistoWiz Inc. (histowiz.com) for histology using a Standard Operating Procedure and fully automated workflow. Samples were processed, embedded in paraffin, sectioned at 4µm and stained using hematoxylin-eosin (H&E). After staining, sections were dehydrated and film coverslipped using a TissueTek-Prisma and Coverslipper (SakuraUSA, Torrance, CA). Whole slide scanning (40x) was performed on an Aperio AT2 (Leica Biosystems, Wetzlar, Germany).

Cytokine Analysis:

Cytokine levels in lung tissues were analyzed using the Bio-Plex Protein Array System (Bio-Rad Laboratories, Hercules, CA). Briefly, lung tissue was excised and homogenized in 2 ml of ice-cold PBS containing 1X Pierce Protease Inhibitor cocktail (Thermo Scientific, Rockford, IL). After a homogenization, Triton X-100 was add to a final concentration of 0.05% and the samples were clarified by centrifugation. Supernatant fractions from the

pulmonary homogenates were then assayed using the Bio-Plex Pro Mouse Cytokine 23-Plex (Bio-Rad Laboratories) for the presence of IL-1α, IL-1β, IL-2, IL-3, IL-4, IL-5, IL-6, IL-9, IL-10, IL-12 (p40), IL-12 (p70), IL-13, IL-17A, granulocyte colony stimulating factor (G-CSF), granulocyte monocyte colony stimulating factor (GM-CSF), interferon-γ (IFN-γ), CXCL1/keratinocyte-derived chemokine (KC), CCL2/monocyte chemotactic protein-1 (MCP-1), CCL3/macrophage inflammatory protein-1α (MIP-1α), CCL4/MIP-1β, CCL5/regulated upon activation, normal T cell expressed and secreted (RANTES) and tumor necrosis factor-α (TNF-α).

Flow Cytometry:

Cell populations in the lungs were identified by flow cytometry. Briefly, lungs from individual mice were enzymatically digested at 37°C for 30 min in digestion buffer (RPMI 1640 containing 1 mg/ml of collagenase type IV). The digested tissues were then successively passed through sterile 70 and 40 µm pore nylon strainers (BD Biosciences, San Jose, CA). Erythrocytes in the strained suspension were lysed by incubation in NH_4Cl buffer (0.859% NH_4Cl, 0.1% $KHCO_3$, 0.0372% Na_2EDTA; pH 7.4; Sigma-Aldrich) for 3 min on ice, followed by the addition of a 2-fold excess of PBS. The leukocytes were then collected by centrifugation, resuspended in sterile PBS, and were stained using the LIVE/DEAD™ Fixable Blue Dead Cell Stain Kit (1:1000; Invitrogen, Carlsbad, CA) for 30 min at 4° C in the dark. Following incubation, samples were washed and resuspended FACS buffer (PBS, 0.1% BSA, 0.02%NaN_3, 2mM EDTA) and incubated with CD16/CD32 (Fc Block™; BD Biosciences, San Jose, CA) for 5 min. For flow cytometry, $1x10^6$ cells were incubated for 30 min at 4° C in the dark with optimal concentrations of fluorochrome-conjugated antibodies (Table S2 for antigen, clone and source) diluted in Brilliant Stain

Buffer (BD Biosciences). After three washes with FACS buffer, the cells were fixed in 2% ultrapure paraformaldehyde. For data acquisition, >200,000 events were collected on a BD LSRFortessa X-20 flow cytometer (BD Biosciences, San Jose, CA), and the data were analyzed with FlowJo V10 (TreeStar, Ashland, OR). The absolute number of cells in each leukocyte subset was determined by multiplying the absolute number of $CD45^+$ cells by the percentage of cells stained by fluorochrome-labeled antibodies for each cell population analyzed.

Neutrophil depletion:

Mice were depleted of neutrophils via intraperitoneal (ip) administration of 200 µg anti-Ly6G (clone 1A8; BioXcell) in 100 µl. Control mice received 200 µg IgG2a isotype control antibody (clone 2A3; BioXcell) in 100 µl. Depletions were started 24 hours prior to challenge and the mice were injected every 24 hours for the first 5 days post challenge. After day 5, the mice were injected every 48 hours.

Statistics:

Data were analyzed using GraphPad Prism, version 8.0 (GraphPad Software, Inc., La Jolla, CA). The one-way analysis of variance (ANOVA) with the Tukey's multiple-correction test was used to compare more than two groups. Kaplan-Meier survival curves were compared using the Mantel-Cox log rank test. p values <0.05 were considered significant.

Acknowledgments:

This work was funded by National Institutes of Health grants AI072195 and AI125045 to JKL. CRH was partly funded by a National Institute of Allergy and Infectious Diseases training grant (T32 AI007172). The funders had no role in study design, data collection and interpretation, or the decision to submit the work for publication.

References:

1. **Andama AO, den Boon S, Meya D, Cattamanchi A, Worodria W, Davis JL, Walter ND, Yoo SD, Kalema N, Haller B, Huang L, International HIVAOPS.** 2013. Prevalence and outcomes of cryptococcal antigenemia in HIV-seropositive patients hospitalized for suspected tuberculosis in Uganda. J Acquir Immune Defic Syndr **63:**189-194.
2. **Denning DW.** 2016. Minimizing fungal disease deaths will allow the UNAIDS target of reducing annual AIDS deaths below 500 000 by 2020 to be realized. Philos Trans R Soc Lond B Biol Sci **371**.
3. **Heitman J, Kozel TR, Kwon-Chung KJ, Perfect JR, Casadevall A.** 2010. *Cryptococcus*: from human pathogen to model yeast. ASM press.
4. **Jarvis JN, Bicanic T, Loyse A, Namarika D, Jackson A, Nussbaum JC, Longley N, Muzoora C, Phulusa J, Taseera K, Kanyembe C, Wilson D, Hosseinipour MC, Brouwer AE, Limmathurotsakul D, White N, van der Horst C, Wood R, Meintjes G, Bradley J, Jaffar S, Harrison T.** 2014. Determinants of mortality in a combined cohort of 501 patients with HIV-associated Cryptococcal meningitis: implications for improving outcomes. Clinical

Infectious Diseases : an official publication of the Infectious Diseases Society of America **58:**736-745.

5. **Rajasingham R, Smith RM, Park BJ, Jarvis JN, Govender NP, Chiller TM, Denning DW, Loyse A, Boulware DR.** 2017. Global burden of disease of HIV-associated cryptococcal meningitis: an updated analysis. Lancet Infect Dis **17:**873-881.

6. **Pyrgos V, Seitz AE, Steiner CA, Prevots DR, Williamson PR.** 2013. Epidemiology of cryptococcal meningitis in the US: 1997-2009. PLoS One **8:**e56269.

7. **Elieh Ali Komi D, Sharma L, Dela Cruz CS.** 2018. Chitin and Its Effects on Inflammatory and Immune Responses. Clin Rev Allergy Immunol **54:**213-223.

8. **Banks IR, Specht CA, Donlin MJ, Gerik KJ, Levitz SM, Lodge JK.** 2005. A chitin synthase and its regulator protein are critical for chitosan production and growth of the fungal pathogen *Cryptococcus neoformans*. Eukaryot Cell **4:**1902-1912.

9. **Baker LG, Specht CA, Lodge JK.** 2011. Cell wall chitosan is necessary for virulence in the opportunistic pathogen *Cryptococcus neoformans*. Eukaryot Cell **10:**1264-1268.

10. **Upadhya R, Lam WC, Maybruck B, Specht CA, Levitz SM, Lodge JK.** 2016. Induction of Protective Immunity to Cryptococcal Infection in Mice by a Heat-Killed, Chitosan-Deficient Strain of *Cryptococcus neoformans*. MBio **7**.

11. **Huffnagle GB, Boyd MB, Street NE, Lipscomb MF.** 1998. IL-5 is required for eosinophil recruitment, crystal deposition, and mononuclear cell recruitment

during a pulmonary *Cryptococcus neoformans* infection in genetically susceptible mice (C57BL/6). J Immunol **160:**2393-2400.

12. **Casadevall A, Pirofski LA.** 2003. The damage-response framework of microbial pathogenesis. Nat Rev Microbiol **1:**17-24.

13. **Wozniak KL, Kolls JK, Wormley FL, Jr.** 2012. Depletion of neutrophils in a protective model of pulmonary cryptococcosis results in increased IL-17A production by gammadelta T cells. BMC Immunol **13:**65.

14. **Leopold Wager CM, Hole CR, Campuzano A, Castro-Lopez N, Cai H, Caballero Van Dyke MC, Wozniak KL, Wang Y, Wormley FL, Jr.** 2018. IFN-gamma immune priming of macrophages in vivo induces prolonged STAT1 binding and protection against *Cryptococcus neoformans*. PLoS Pathog **14:**e1007358.

15. **Delliere S, Guery R, Candon S, Rammaert B, Aguilar C, Lanternier F, Chatenoud L, Lortholary O.** 2018. Understanding Pathogenesis and Care Challenges of Immune Reconstitution Inflammatory Syndrome in Fungal Infections. J Fungi (Basel) **4**.

16. **Haddow LJ, Colebunders R, Meintjes G, Lawn SD, Elliott JH, Manabe YC, Bohjanen PR, Sungkanuparph S, Easterbrook PJ, French MA, Boulware DR, International Network for the Study of HIVal.** 2010. Cryptococcal immune reconstitution inflammatory syndrome in HIV-1-infected individuals: proposed clinical case definitions. Lancet Infect Dis **10:**791-802.

17. **Boulware DR, Meya DB, Bergemann TL, Wiesner DL, Rhein J, Musubire A, Lee SJ, Kambugu A, Janoff EN, Bohjanen PR.** 2010. Clinical features and

476 serum biomarkers in HIV immune reconstitution inflammatory syndrome after
477 cryptococcal meningitis: a prospective cohort study. PLoS Med **7:**e1000384.
478 18. **O'Meara TR, Holmer SM, Selvig K, Dietrich F, Alspaugh JA.** 2013.
479 *Cryptococcus neoformans* Rim101 is associated with cell wall remodeling and
480 evasion of the host immune responses. MBio **4**.
481 19. **Ellerbroek PM, Lefeber DJ, van Veghel R, Scharringa J, Brouwer E, Gerwig**
482 **GJ, Janbon G, Hoepelman AI, Coenjaerts FE.** 2004. O-acetylation of
483 cryptococcal capsular glucuronoxylomannan is essential for interference with
484 neutrophil migration. J Immunol **173:**7513-7520.
485 20. **Coenjaerts FE, Walenkamp AM, Mwinzi PN, Scharringa J, Dekker HA, van**
486 **Strijp JA, Cherniak R, Hoepelman AI.** 2001. Potent inhibition of neutrophil
487 migration by cryptococcal mannoprotein-4-induced desensitization. J Immunol
488 **167:**3988-3995.
489 21. **Rocha JD, Nascimento MT, Decote-Ricardo D, Corte-Real S, Morrot A,**
490 **Heise N, Nunes MP, Previato JO, Mendonca-Previato L, DosReis GA,**
491 **Saraiva EM, Freire-de-Lima CG.** 2015. Capsular polysaccharides from
492 *Cryptococcus neoformans* modulate production of neutrophil extracellular traps
493 (NETs) by human neutrophils. Sci Rep **5:**8008.
494 22. **Zhang M, Sun D, Liu G, Wu H, Zhou H, Shi M.** 2016. Real-time in vivo imaging
495 reveals the ability of neutrophils to remove *Cryptococcus neoformans* directly
496 from the brain vasculature. J Leukoc Biol **99:**467-473.
497 23. **Sun D, Zhang M, Liu G, Wu H, Li C, Zhou H, Zhang X, Shi M.** 2016.
498 Intravascular clearance of disseminating *Cryptococcus neoformans* in the brain

can be improved by enhancing neutrophil recruitment in mice. Eur J Immunol **46:**1704-1714.

24. **Mednick AJ, Feldmesser M, Rivera J, Casadevall A.** 2003. Neutropenia alters lung cytokine production in mice and reduces their susceptibility to pulmonary cryptococcosis. Eur J Immunol **33:**1744-1753.

25. **Wiesner DL, Smith KD, Kashem SW, Bohjanen PR, Nielsen K.** 2017. Different Lymphocyte Populations Direct Dichotomous Eosinophil or Neutrophil Responses to Pulmonary *Cryptococcus* Infection. J Immunol **198:**1627-1637.

26. **Davidson RC, Blankenship JR, Kraus PR, de Jesus Berrios M, Hull CM, D'Souza C, Wang P, Heitman J.** 2002. A PCR-based strategy to generate integrative targeting alleles with large regions of homology. Microbiology **148:**2607-2615.

27. **Gerik KJ, Donlin MJ, Soto CE, Banks AM, Banks IR, Maligie MA, Selitrennikoff CP, Lodge JK.** 2005. Cell wall integrity is dependent on the PKC1 signal transduction pathway in *Cryptococcus neoformans*. Mol Microbiol **58:**393-408.

28. **Toffaletti DL, Rude TH, Johnston SA, Durack DT, Perfect JR.** 1993. Gene transfer in *Cryptococcus neoformans* by use of biolistic delivery of DNA. J Bacteriol **175:**1405-1411.

29. **Gerik KJ, Bhimireddy SR, Ryerse JS, Specht CA, Lodge JK.** 2008. PKC1 is essential for protection against both oxidative and nitrosative stresses, cell integrity, and normal manifestation of virulence factors in the pathogenic fungus *Cryptococcus neoformans*. Eukaryot Cell **7:**1685-1698.

30. **Upadhya R, Baker LG, Lam WC, Specht CA, Donlin MJ, Lodge JK.** 2018. *Cryptococcus neoformans* Cda1 and Its Chitin Deacetylase Activity Are Required for Fungal Pathogenesis. MBio **9**.

31. **Smith RL, Gilkerson E.** 1979. Quantitation of glycosaminoglycan hexosamine using 3-methyl-2-benzothiazolone hydrazone hydrochloride. Anal Biochem **98:**478-480.

Figure legends:

Figure 1. Deletion and complementation of *C. neoformans* chitin synthase 3 (Chs3): (A) For morphological analysis, cells were incubated for 2 days in YPD and diluted to an OD_{650} of 0.2 with PBS. Five microliters each cell solution was spotted on to a clean glass slide and photographed at 40X. (B) Temperature sensitivity. Cultures were grown overnight in YPD then diluted to an OD650 of 1.0. Tenfold serial dilutions were made in PBS and 3µl of each was plated. The plates were grown for 4 days at 30°C or 39°C. (C) Quantitative determination of cell wall chitosan by the MBTH assay. Cells were grown in YPD for two days, collected, washed and used for the assay. Data represents the average of three biological experiments ± standard deviation (SD) and are expressed as nMoles of glucosamine per mg dry weight of yeast cells (***, $P < 0.001$).

Figure 2. Inoculation with the *chs3*Δ strain induces rapid mouse mortality: C57BL/6 mice were infected with 10^7 live CFUs of each strain by intranasal inoculation. Survival of the animals was recorded as mortality of mice for 40 days post inoculation. Mice that lost

544 20% of the body weight at the time of inoculation or displayed signs of morbidity were
545 considered ill and sacrificed. Data is representative of one experiment with 5 mice for
546 KN99, 5 mice for *cda1Δ2Δ3Δ,* 10 mice for *chs3*Δ, and 10 mice for *chs3*Δ*::CHS3*. Virulence
547 was determined using Mantel-Cox curve comparison with statistical significance
548 determined by log-rank test. (***, $P < 0.001$).

549 **Figure 3. Mortality is not dependent on the viability of the fungi or mouse**
550 **background:** (A) C57BL/6, (B) BALB/c, or (C) CBA/J mice were inoculated with 10^7 Heat-
551 killed CFUs of each strain by intranasal inoculation. Survival of the animals was recorded
552 as mortality of mice for 20 days post inoculation. Mice that lost 20% of the body weight at
553 the time of inoculation or displayed signs of morbidity were considered ill and sacrificed.
554 Data is cumulative of one experiment with 5 mice for KN99, and two experiments with 5
555 mice for *chs3*Δ and *chs3*Δ*::CHS3* each for a total of 10 mice. Virulence was determined
556 using Mantel-Cox curve comparison with statistical significance determined by log-rank
557 test. (***, $P < 0.001$).

558 **Figure 4. Massive inflammatory response is triggered to *chs3*Δ*:*** C57BL/6 mice were
559 inoculated with 10^7 Heat-killed CFUs of each strain by intranasal inoculation. At 8 hours
560 post inoculation, the lungs were harvested, embedded, sectioned and processed for
561 hematoxylin-eosin staining. HK KN99 inoculated mice (A-C) display a limited
562 inflammatory response. HK *chs3*Δ inoculated mice (D-F) exhibit abundant foci of
563 inflammation (black arrows) spread across the whole lung section consisting of a
564 profound amount of mixed inflammatory infiltrates with enhanced presences of
565 neutrophils (green arrows). HK *chs3*Δ*::CHS3* inoculated mice (G-I) displayed a similar

566 limited inflammatory response observed in the HK KN99 inoculated mice. Images are
567 representative images of two independent experiments using three mice per group.

568 **Figure 5. *chs3*Δ induces a strong proinflammatory cytokine response:** C57BL/6 mice
569 were inoculated with 10^7 Heat-killed CFUs of each strain by intranasal inoculation. At 8
570 hours post inoculation, homogenates were prepared from the lungs of each group.
571 Cytokine/chemokine responses were determined from the lung homogenates using the
572 Bio-Plex Protein Array System. Data is cumulative of one experiment with 5 mice for PBS
573 and KN99, and two experiments with 5 mice for *chs3*Δ and *chs3*Δ*::CHS3* each for a total
574 of 10 mice experiments, ± standard errors of the means (SEM). Each dot represents data
575 from an individual mouse. (***, $P < 0.001$)

576 **Figure 6. A significant increase in neutrophil recruitment in *chs3*Δ inoculated mice.**
577 C57BL/6 mice were inoculated with 10^7 Heat-killed CFUs of each strain by intranasal
578 inoculation. At 8 hours post inoculation, pulmonary leukocytes were isolated from the lungs
579 of each group and subjected to flow cytometry analysis (see Supplemental Table 2 for
580 antibodies and Supplemental Fig. 3 for gating strategy). (A) total cell number of leukocytes.
581 (B) Total and (C) percent neutrophils ($CD11b^+/CD24^+/Ly6G^+/CD45^+$). Data is cumulative of
582 one experiment with 5 mice for PBS and KN99, and two experiments with 5 mice for *chs3*Δ
583 and *chs3*Δ*::CHS3* each for a total of 10 mice experiments, ± standard errors of the means
584 (SEM). Each dot represents data from an individual mouse. (***, $P < 0.001$)

585 **Figure 7. Depletion of neutrophils protects *chs3*Δ inoculated mice:** (A) C57BL/6, (B)
586 BALB/c, or (C) CBA/J mice were inoculated with 10^7 Heat-killed CFUs of each strain by
587 intranasal inoculation. Prior to inoculation and throughout the experiment, mice were
588 treated with isotype antibody or anti-Ly6G antibody. Survival of the animals was recorded

as mortality of mice for 20 days post inoculation. Mice that lost 20% of the body weight at the time of inoculation or displayed signs of morbidity were considered ill and sacrificed. Data is cumulative of two independent experiments with 5 mice for *chs3*Δ and *chs3*Δ*::CHS3* each for a total of 10 mice. Virulence was determined using Mantel-Cox curve comparison with statistical significance determined by log-rank test. (***, $P < 0.001$).

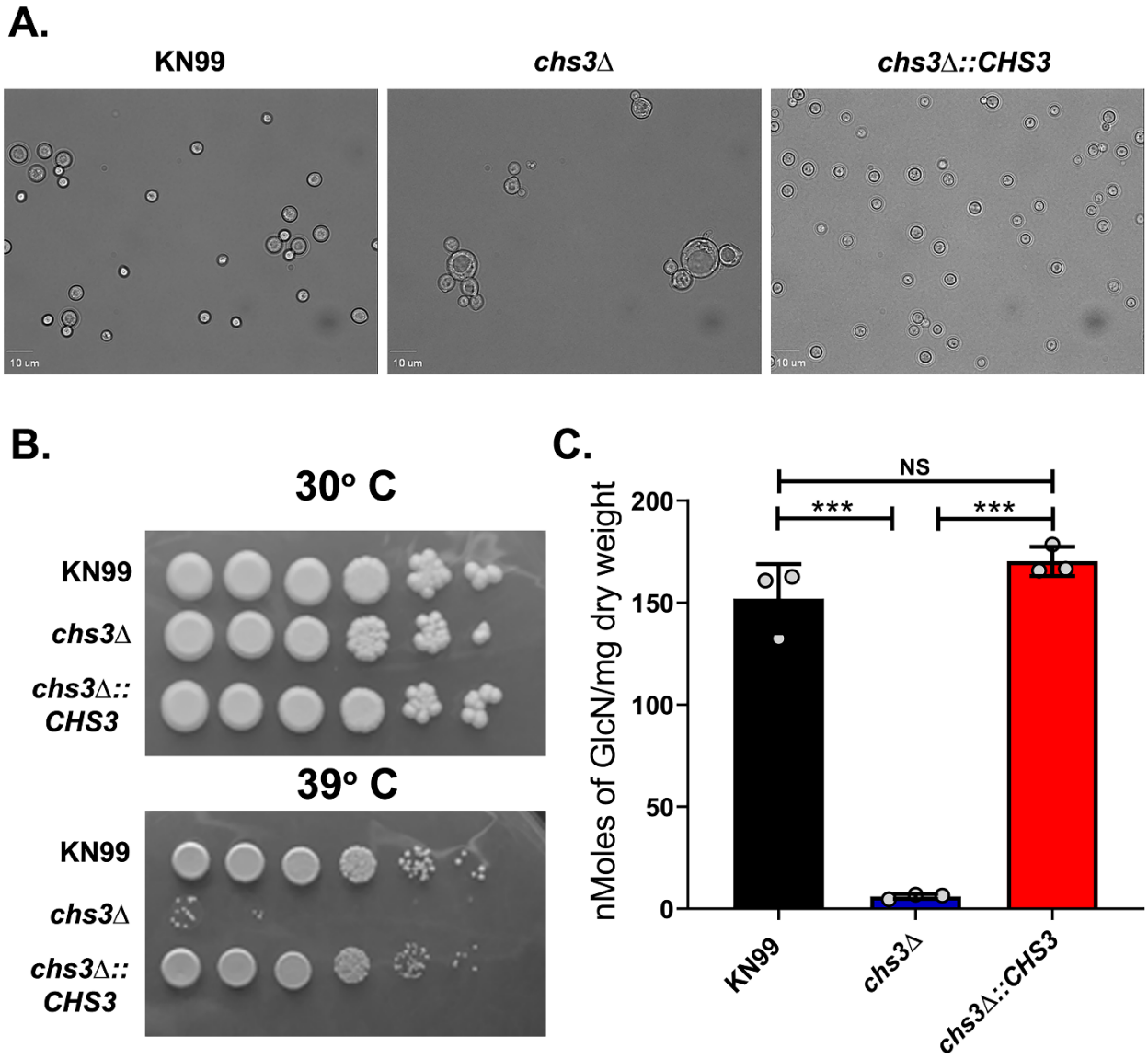

Figure 1. Deletion and complementation of *C. neoformans* chitin synthase 3 (Chs3): (A) For morphological analysis, cells were incubated for 2 days in YPD and diluted to an OD_{650} of 0.2 with PBS. Five microliters each cell solution was spotted on to a clean glass slide and photographed at 40X. (B) Temperature sensitivity. Cultures were grown overnight in YPD then diluted to an OD650 of 1.0. Tenfold serial dilutions were made in PBS and 3µl of each was plated. The plates were grown for 4 days at 30°C or 39°C. (C) Quantitative determination of cell wall chitosan by the MBTH assay. Cells were grown in YPD for two days, collected, washed and used for the assay. Data represents the average of three biological experiments ± standard deviation (SD) and are expressed as nMoles of glucosamine per mg dry weight of yeast cells (***, $P < 0.001$).

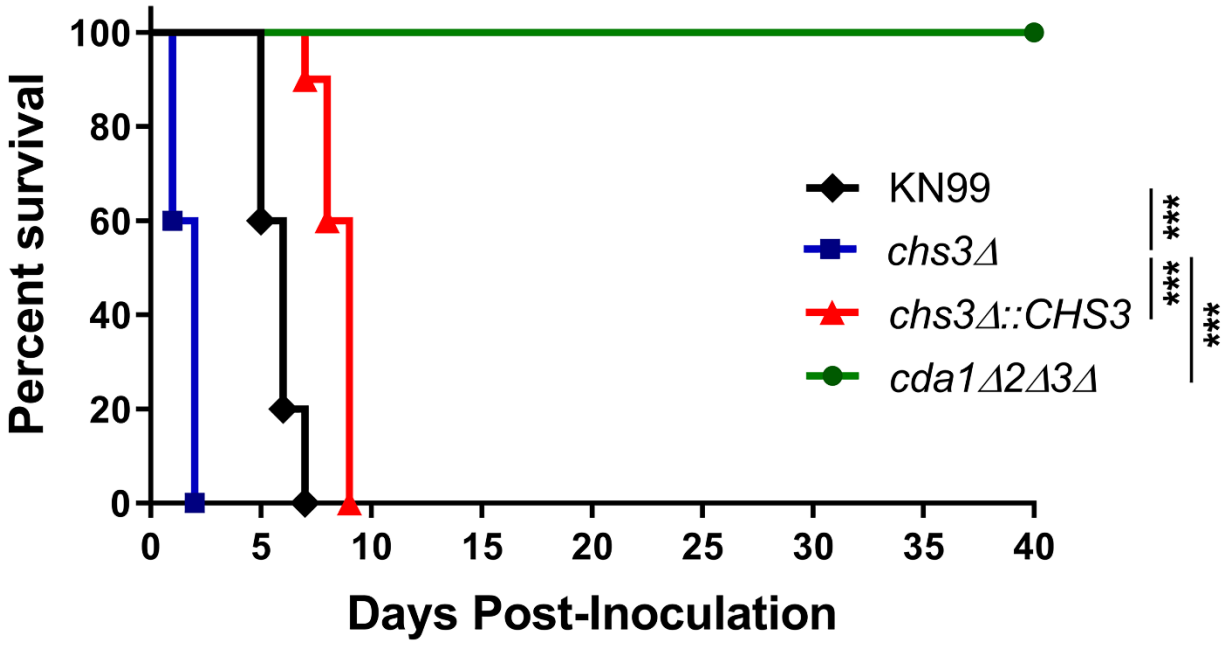

Figure 2. Inoculation with the *chs3*Δ strain induces rapid mouse mortality: C57BL/6 mice were infected with 10^7 live CFUs of each strain by intranasal inoculation. Survival of the animals was recorded as mortality of mice for 40 days post inoculation. Mice that lost 20% of the body weight at the time of inoculation or displayed signs of morbidity were considered ill and sacrificed. Data is representative of one experiment with 5 mice for KN99, 5 mice for *cda1Δ2Δ3Δ,* 10 mice for *chs3*Δ, and 10 mice for *chs3*Δ*::CHS3*. Virulence was determined using Mantel-Cox curve comparison with statistical significance determined by log-rank test. (***, $P < 0.001$).

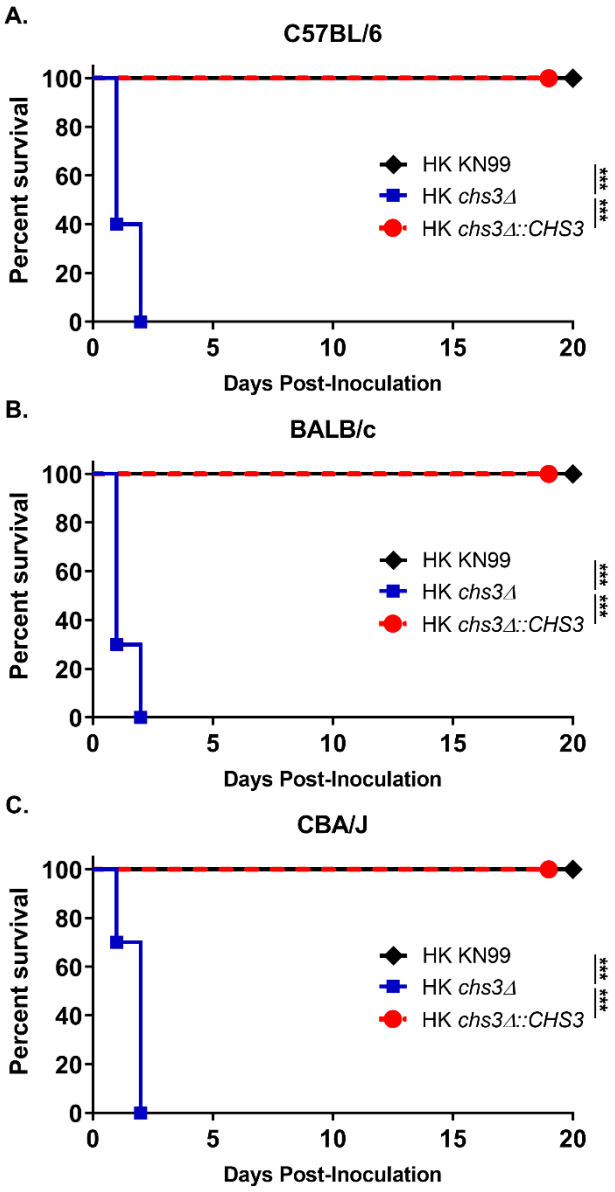

Figure 3. Mortality is not dependent on the viability of the fungi or mouse background: (A) C57BL/6, (B) BALB/c, or (C) CBA/J mice were inoculated with 10^7 Heat-killed CFUs of each strain by intranasal inoculation. Survival of the animals was recorded as mortality of mice for 20 days post inoculation. Mice that lost 20% of the body weight at the time of inoculation or displayed signs of morbidity were considered ill and sacrificed. Data is cumulative of one experiment with 5 mice for KN99, and two experiments with 5 mice for *chs3*Δ and *chs3*Δ*::CHS3* each for a total of 10 mice. Virulence was determined using Mantel-Cox curve comparison with statistical significance determined by log-rank test. (***, $P < 0.001$).

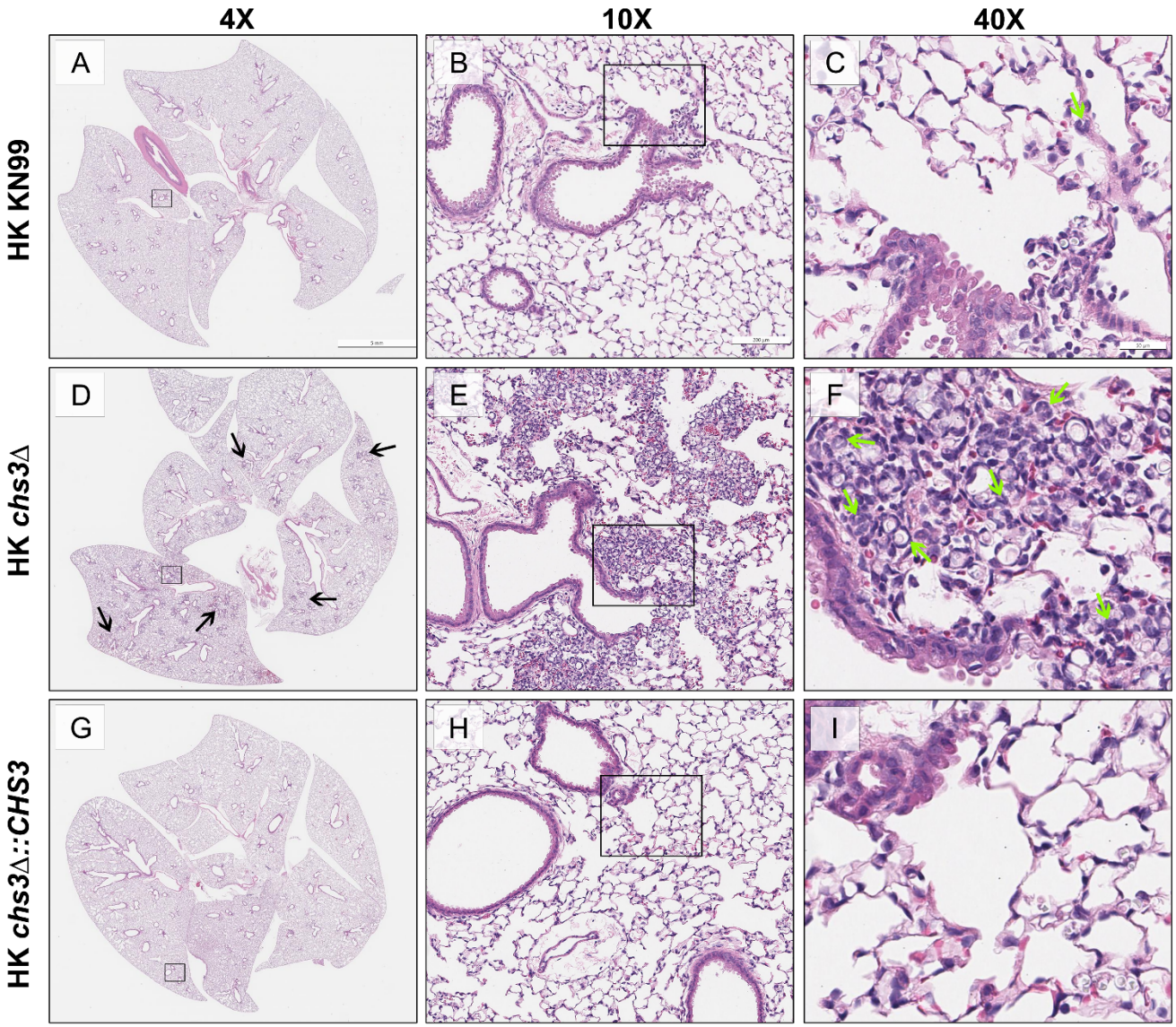

Figure 4. Massive inflammatory response is triggered to *chs3*Δ*:* C57BL/6 mice were inoculated with 10^7 Heat-killed CFUs of each strain by intranasal inoculation. At 8 hours post inoculation, the lungs were harvested, embedded, sectioned and processed for hematoxylin-eosin staining. HK KN99 inoculated mice (A-C) display a limited inflammatory response. HK *chs3*Δ inoculated mice (D-F) exhibit abundant foci of inflammation (black arrows) spread across the whole lung section consisting of a profound amount of mixed inflammatory infiltrates with enhanced presences of neutrophils (green arrows). HK *chs3*Δ*::CHS3* inoculated mice (G-I) displayed a similar limited inflammatory response observed in the HK KN99 inoculated mice. Images are representative images of two independent experiments using three mice per group.

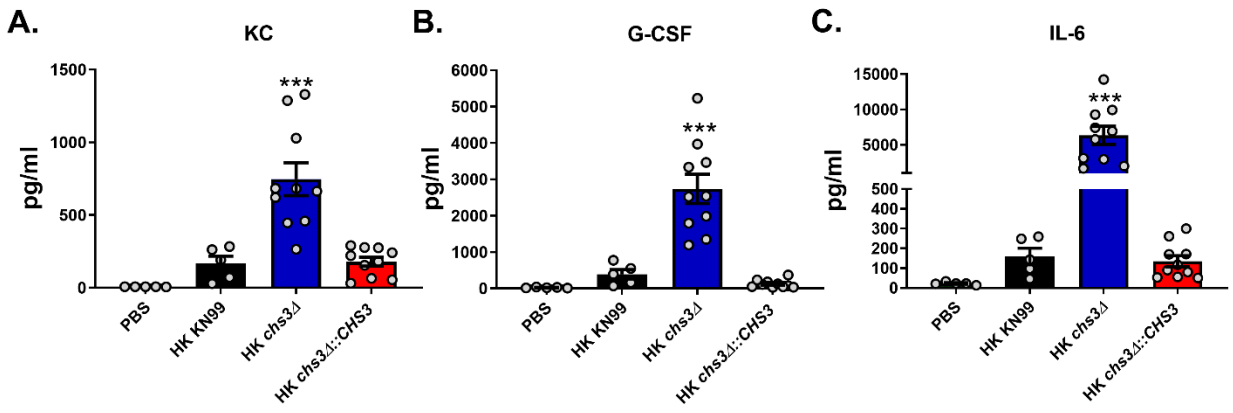

Figure 5. *chs3*Δ induces a strong proinflammatory cytokine response: C57BL/6 mice were inoculated with 10^7 Heat-killed CFUs of each strain by intranasal inoculation. At 8 hours post inoculation, homogenates were prepared from the lungs of each group. Cytokine/chemokine responses were determined from the lung homogenates using the Bio-Plex Protein Array System. Data is cumulative of one experiment with 5 mice for PBS and KN99, and two experiments with 5 mice for *chs3*Δ and *chs3*Δ*::CHS3* each for a total of 10 mice experiments, ± standard errors of the means (SEM). Each dot represents data from an individual mouse. (***, $P < 0.001$)

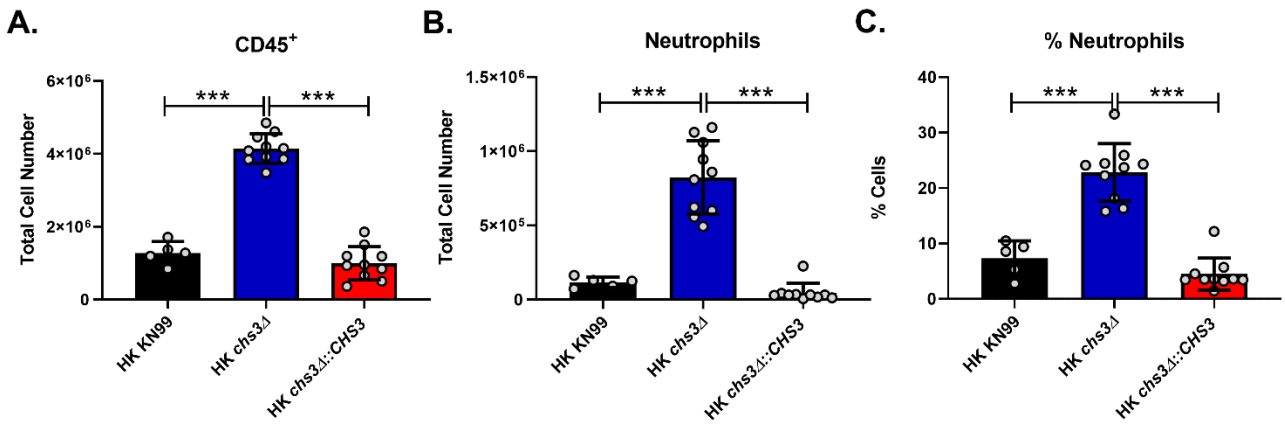

Figure 6. A significant increase in neutrophil recruitment in *chs3*Δ inoculated mice. C57BL/6 mice were inoculated with 10^7 Heat-killed CFUs of each strain by intranasal inoculation. At 8 hours post inoculation, pulmonary leukocytes were isolated from the lungs of each group and subjected to flow cytometry analysis (see Supplemental Table 2 for antibodies and Supplemental Fig. 3 for gating strategy). (A) total cell number of leukocytes. (B) Total and (C) percent neutrophils ($CD11b^+/CD24^+/Ly6G^+/CD45^+$). Data is cumulative of one experiment with 5 mice for PBS and KN99, and two experiments with 5 mice for *chs3*Δ and *chs3*Δ*::CHS3* each for a total of 10 mice experiments, ± standard errors of the means (SEM). Each dot represents data from an individual mouse. (***, $P < 0.001$)

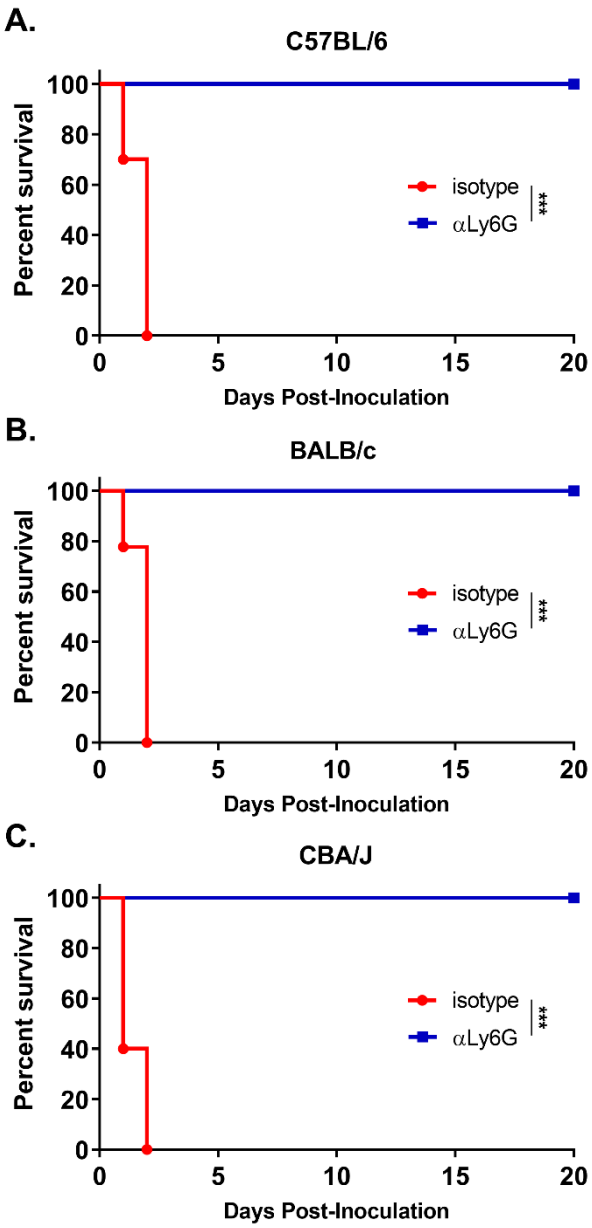

Figure 7. Depletion of neutrophils protects *chs3*Δ inoculated mice: (A) C57BL/6, (B) BALB/c, or (C) CBA/J mice were inoculated with 10^7 Heat-killed CFUs of each strain by intranasal inoculation. Prior to inoculation and throughout the experiment, mice were treated with isotype antibody or anti-Ly6G antibody. Survival of the animals was recorded as mortality of mice for 20 days post inoculation. Mice that lost 20% of the body weight at the time of inoculation or displayed signs of morbidity were considered ill and sacrificed. Data is cumulative of two independent experiments with 5 mice for *chs3*Δ and *chs3*Δ*::CHS3* each for a total of 10 mice. Virulence was determined using Mantel-Cox curve comparison with statistical significance determined by log-rank test. (***, $P < 0.001$).

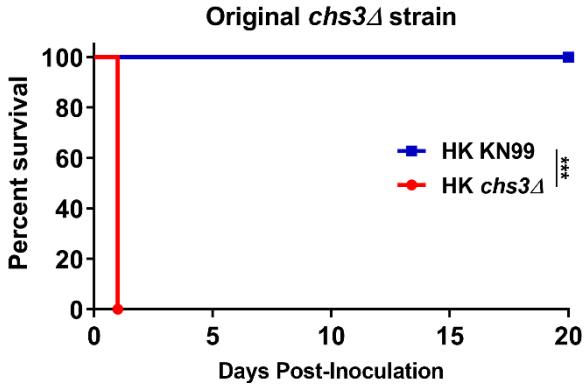

Supplemental figure 1: The original *chs3*Δ strain also induces rapid mortality: C57BL/6 mice were inoculated with 10^7 Heat-killed CFUs of each strain by intranasal inoculation. Survival of the animals was recorded as mortality of mice for 20 days post inoculation. Mice that lost 20% of the body weight at the time of inoculation or displayed signs of morbidity were considered ill and sacrificed. Data is representative of one experiment with 5 mice for each strain. Virulence was determined using Mantel-Cox curve comparison with statistical significance determined by log-rank test. (***, $P < 0.001$).

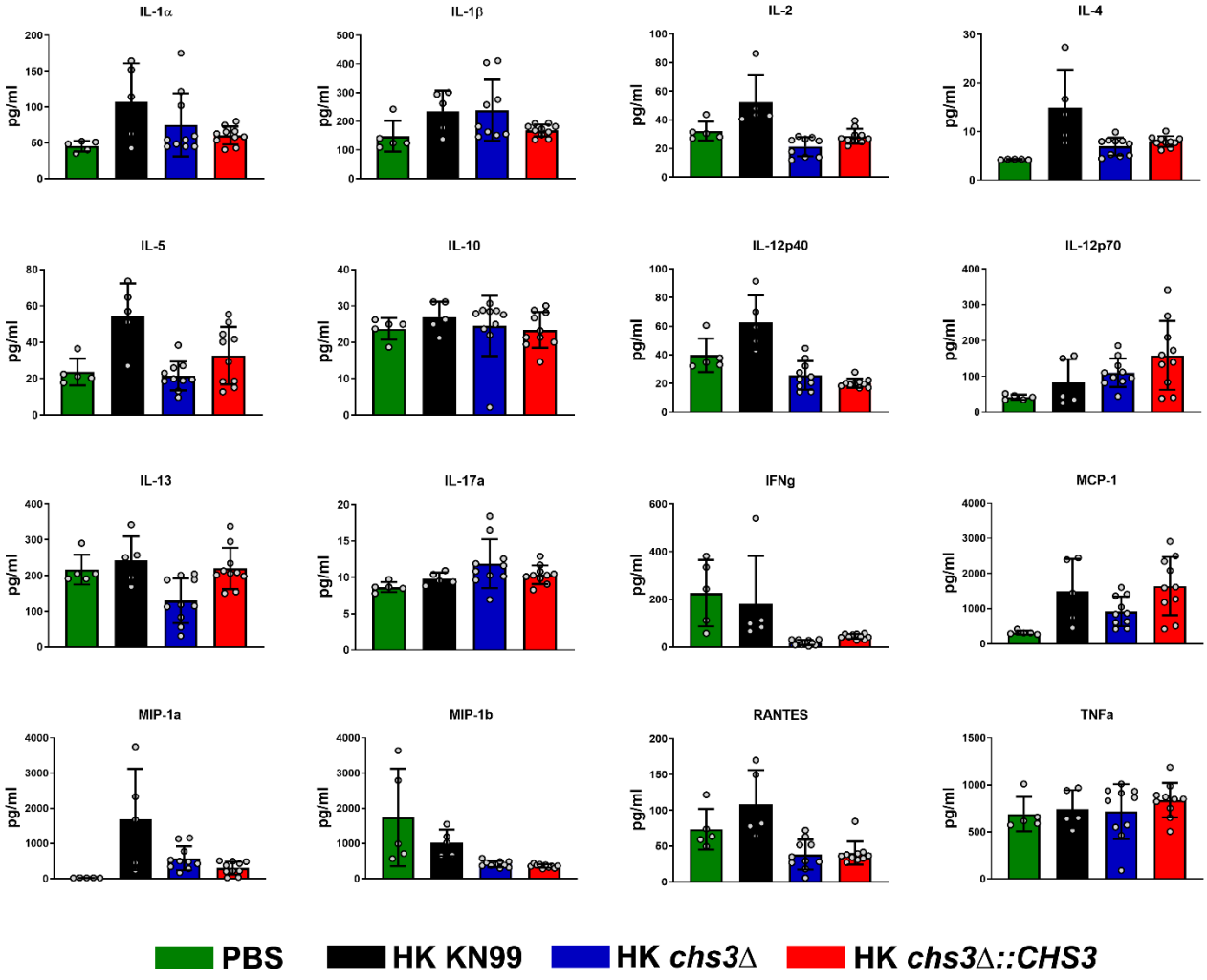

Supplemental figure 2. Cytokine/chemokine analysis: C57BL/6 mice were inoculated with 10^7 Heat-killed CFUs of each strain by intranasal inoculation. At 8 hours post inoculation, homogenates were prepared from the lungs of each group. Cytokine/chemokine responses were determined from the lung homogenates using the Bio-Plex Protein Array System. Data is cumulative of one experiment with 5 mice for PBS and KN99, and two experiments with 5 mice for *chs3*Δ and *chs3*Δ*::CHS3* each for a total of 10 mice experiments, ± standard errors of the means (SEM). Each dot represents data from an individual mouse.

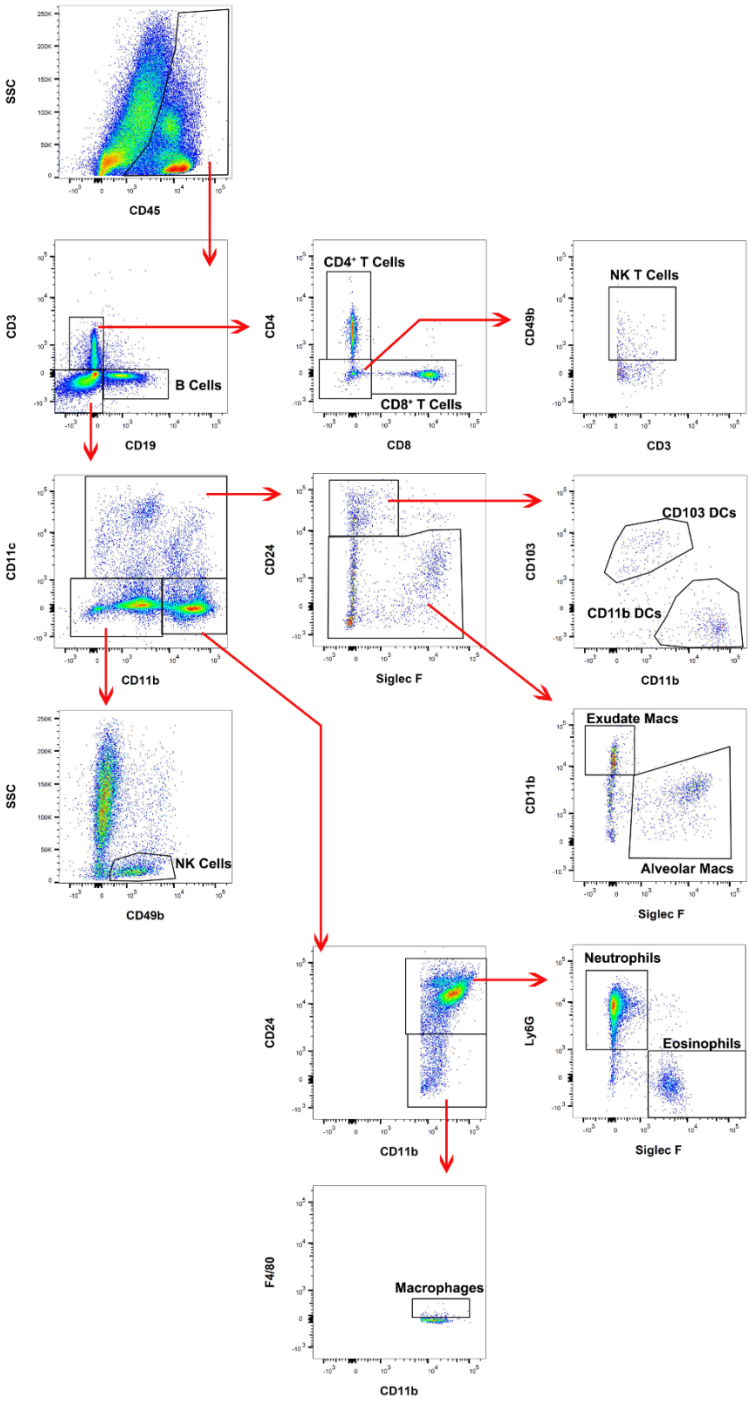

Supplemental figure 3. Flow cytometry gating strategy. Flow cytometry analysis of host leukocyte populations in C57BL/6 mice 8 hours post inoculation with 10^7 Heat-killed CFUs of *chs3*Δ. After separation based on physical properties to eliminate debris and doublets, dead cells were excluded by live/dead staining (not shown). CD45+ cells (leukocytes; top left) were subjected to analysis based on their expression of CD3, CD4, CD8a, CD11b, CD11c, CD19, CD24, CD49b, CD103, F4/80, Ly-6G, and Siglec F. The specific populations of cells identified are indicated on the flow plots.

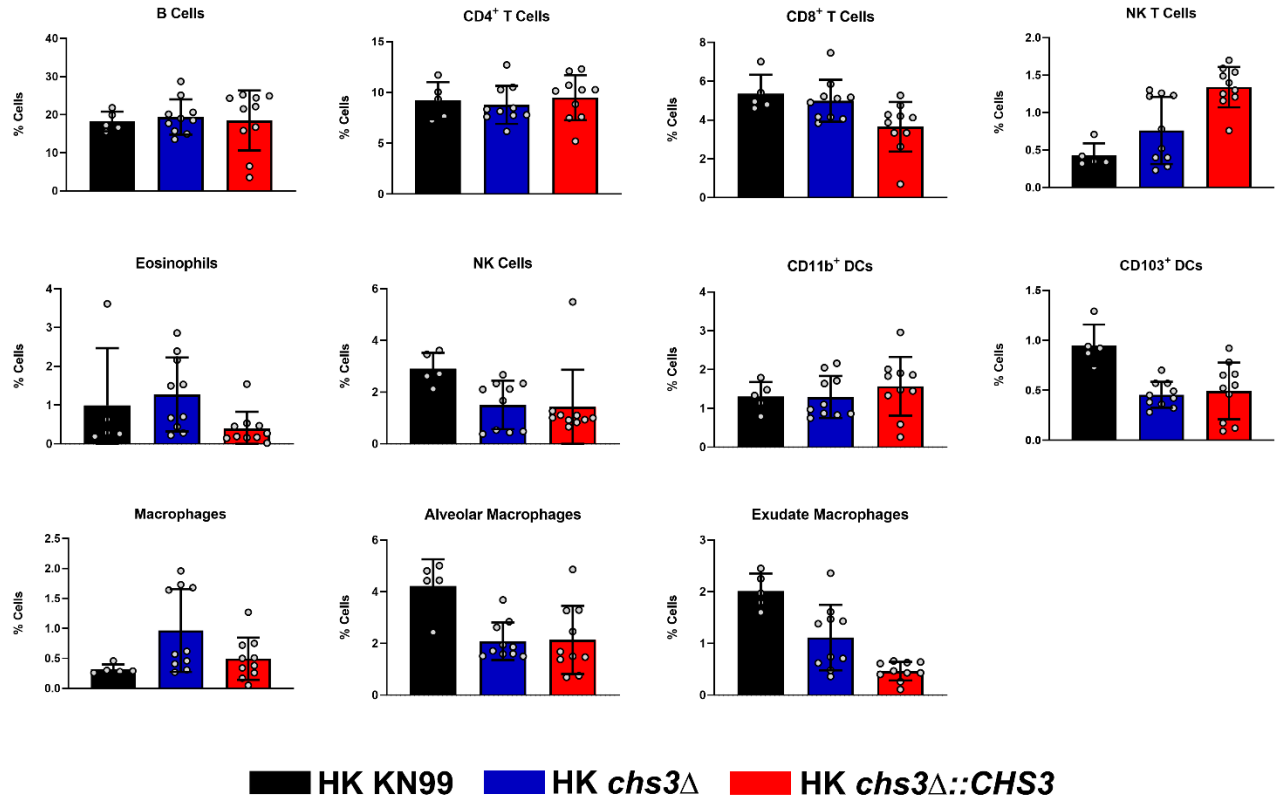

Supplemental figure 4. Flow cytometry analysis: C57BL/6 mice were inoculated with 10^7 Heat-killed CFUs of each strain by intranasal inoculation. At 8 hours post inoculation, pulmonary leukocytes were isolated from the lungs of each group and subjected to flow cytometry analysis Data is cumulative of one experiment with 5 mice for PBS and KN99, and two experiments with 5 mice for *chs3*Δ and *chs3*Δ*::CHS3* each for a total of 10 mice experiments, ± standard errors of the means (SEM). Each dot represents data from an individual mouse.

Table S1. Primer used in this study.

Primer	Sequence
Chs3-1	CGTCAACCCAACCACATTC
Chs3-2	CAGCTCTCAGATCACGTTTACCT
Chs3-3	CGGAAATTGCTGCTCCCTAcaggaaacagctatgaccatg
Chs3-4	catggtcatagctgtttcctgTAGGGAGCAGCAATTTCCG
Chs3-5	cactggccgtcgttttacaacGCGGATAAACATCCGTCAAAG
Chs3-6	CTTTGACGGATGTTTATCCGCgttgtaaaacgacggccagtg
Chs3-7	GAAAAGTTGAAGAAAAGGATCAATACC
Chs3-8	CTCTCAACTGTTTTAATCAACGAATG
Chs3-9	GACACGTTCTGTTGGAGATGG
Chs3-10	CTGTAAGTTCCTAACGCGAAACG

Table S2. Antibodies for flow analysis.

Antigen	Clone	Fluorophore	Dilution	Company
CD3	17-A2	APC-Cy7	1:250	BioLegend
CD4	GK1.5	BUV737	1:500	BD Biosciences
CD8a	53-6.7	BV650	1:125	BD Biosciences
CD11b	M1/70	BV510	1:250	BD Biosciences
CD11c	N418	PE	1:125	Invitrogen
CD16/CD32 Fc Block	2.4G2	(not applicable)	1:500	BD Biosciences
CD19	1D3	BV786	1:125	BD Biosciences
CD24	M1/69	PerCP-Cy5.5	1:125	BD Biosciences
CD45	30-F11	Pacific Blue	1:250	BioLegend
CD49b	DX5	PE-Cy7	1:250	Invitrogen
CD103	2E7	Alexa488	1:125	BioLegend
F4/80	BM8	APC	1:250	Invitrogen
Ly6G	1A8	BV711	1:125	BD Biosciences
Siglec-F	E50-2440	PE-CF594	1:250	BD Biosciences